Visual data mining with self-organising maps for ventricular fibrillation analysis

Alfredo Rosado-Muñoz[a], José M. Martínez-Martínez[b,*], Pablo Escandell-Montero[b], Emilio Soria-Olivas[b]

[a] GPDS, Grupo de Procesado Digital de Señales, University of Valencia – Electronic Engineering Department, Av de la Universidad, s/n, 46100 Burjassot, Valencia, Spain
[b] IDAL, Intelligent Data Analysis Laboratory, University of Valencia – Electronic Engineering Department, Av de la Universidad, s/n, 46100 Burjassot, Valencia, Spain

ARTICLE INFO

ABSTRACT

Detection of ventricular fibrillation (VF) at an early stage is being deeply studied in order to lower the risk of sudden death and allows the specialist to have greater reaction time to give the patient a good recovering therapy. Some works are focusing on detecting VF based on numerical analysis of time–frequency distributions, but in general the methods used do not provide insight into the problem. However, this study proposes a new methodology in order to obtain information about this problem. This work uses a supervised self-organising map (SOM) to obtain visually information among four important groups of patients: VF (ventricular fibrillation), VT (ventricular tachycardia), HP (healthy patients) and AHR (other anomalous heart rates and noise). A total number of 27 variables were obtained from continuous surface ECG recordings in standard databases (MIT and AHA), providing information in the time, frequency, and time–frequency domains. self-organising maps (SOMs), trained with 11 of the 27 variables, were used to extract knowledge about the variable values for each group of patients. Results show that the SOM technique allows to determine the profile of each group of patients, assisting in gaining a deeper understanding of this clinical problem. Additionally, information about the most relevant variables is given by the SOM analysis.

© 2013 Elsevier Ireland Ltd. All rights reserved.

1. Introduction

Ventricular fibrillation (VF) is a cardiac arrhythmia caused by a disorganised electrical activity of the heart [1] causing collapse and unconsciousness, following a serious risk of death unless an appropriate recovering therapy is applied (typically, a high voltage defibrillation shock) [2]. Clinical and experimental studies have demonstrated that the success of defibrillation is inversely related to the time interval between the beginning of the VF episode and the application of the electrical shock [3–5]. For this reason, the development of early VF detection algorithms for monitoring systems and automatic external defibrillators (AEDs) is being deeply studied. However, in general, these methods do not provide insight into the problem. For this reason, this paper proposes a new methodology in order to obtain visual information about this problem.

Detection algorithms analyse the surface electrocardiogram (ECG), providing a fast and accurate diagnosis of VF in order to reduce the reaction time of specialist in case of monitory systems or even supply the appropriate therapy without the need of qualified personnel as in the case

---

of automatic external defibrillators (AEDs) [6]. Non-invasive detection of VF is typically based on extracting parameters from the ECG signal in different representations such as time, frequency, and time–frequency domains. Time-domain methods analyse the morphology of the ECG to discriminate VF rhythms [7–10]. Frequency-domain measurements are motivated by experimental studies supporting that VF is not a chaotic and disorganised pathology and a certain degree of spatio-temporal organization exists during VF [11–13]. Spectral description of the ECG has revealed important differences between normal and fibrillatory rhythms [12,14,15]. In this context, relevant parameters of the ECG spectrum have been used for developing VF detectors [16–18]. Concerning time–frequency domain, useful information can be extracted given the non-stationary nature of the VF signal, obtaining the continuous temporal evolution of frequency values in the ECG signal and thus, being able to detect changes leading to pathologic rhythms. Algorithms based on time–frequency distributions have also been proposed to detect VF episodes [19–21], and different signal processing techniques are applied by different authors to detect VF accurately [22–25]. An in-depth review of different time, frequency, wavelet and other VF detection methods is described in [26].

The combination of ECG parameters in different domains has been suggested as a useful approach to improve detection efficiency. In [27–29], a set of temporal and spectral features was used as input variables of a neural network, exhibiting better performance than other previously proposed methods. Following this approach, other statistical learning algorithms such as clustering methods [30], support vector machines (SVMs) [31] or data mining procedures [32] have been explored to enhance detection capabilities. This paper makes use of self-organising maps, using also a set of temporal and spectral features as input variables, to obtain visual information about the faced problem.

Self-organising maps (SOMs) are one of the most popular visualization tool nowadays [33]. This neural model is used to find and visualize patterns in N-dimensional data sets. Classical approaches represent the data in two and three dimensions, but when the dimension number is greater than three, it is very complicated to represent the obtained data without establishing any type of restriction as fixing certain set of variables and representing the rest. Such a restriction leads to a partial representation of the information and could hide relevant information. Nevertheless, SOM allow to visualize the data in all the dimensions without any restriction and find patterns in data sets with high dimensionality, maintaining topographical relationships between the original and output spaces. If two patterns are close to each other in the original space, they will also be close in the output space. This paper proposes the use of a supervised SOM to obtain visual information about four important groups of patients: VF (ventricular fibrillation), VT (ventricular tachycardia), HP (healthy patients) and AHR (anomalous heart rates and noise). Moreover, SOM is used to extract knowledge about the variable values and the profile for each group of patients, assisting in gaining a deeper understanding of this clinical problem.

The rest of this paper is organised as follows. The details of the SOM algorithm are described in Section 2. The supervised approach of the SOM algorithm used in this work is
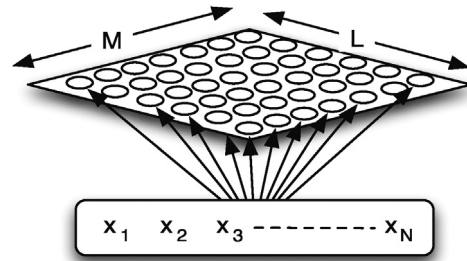

Fig. 1 – Self-organising map scheme.

described in Section 2.2. The aspects related to the dataset used to extract the conclusions are described in Section 3. In Section 4 the results obtained with the data set are presented. Finally, Section 5 summarizes the conclusions of the present work.

2. Self organising map (SOM)

2.1. Classical approach

The Self-organising map (SOM) is a neural network proposed by Kohonen in [34] and, since then, it has been analysed and employed extensively. A recent overview can be found in [35,36]. The SOM and its variants have been employed very often in a wide variety of domains, such as financial [37], medical [38], engineering applications [39,40] and even in the field of animal sciences [41–43]. In an SOM, neurons are arranged in two layers (Fig. 1): an input layer formed by N neurons (one neuron for each input variable) and an output layer where information is processed. This second layer is arranged in a regular low-dimensional grid, usually, a two-dimensional structure.

The number of neurons may vary from a few dozens up to several thousands. Each neuron is represented by an N-dimensional weight vector $m = [m_1, \ldots, m_N]$, where N is equal to the dimension of the input vector. The key of the SOM working principle is to keep a neighbourhood relation between the original space of the N-dimensional data and the regular low-dimensional grid. In the case presented in this paper, this means that similar patient behaviour (as described by the observed variables) are placed in close areas in the mentioned low dimensional grid.

In the SOM design, the main choices are related to the selection of the map type (hexagonal or rectangular grid, which indicates the topology or neighbourhood relation) and the number of neurons (this will define the size of the low-dimensional grid). These choices depend on the number of patterns considered, number of variables defining these patterns and, finally, the existing data dispersion [44].

The next step is to obtain the associated coefficients for each neuron, called synaptic weights. For this purpose, a learning algorithm is used. The first step in this algorithm is the weight initialization. Once the initial values of synaptic weights have been selected, the next step is to get them closer to the optimum values by means of an iterative procedure. In each training step, one sample vector x from the input data set
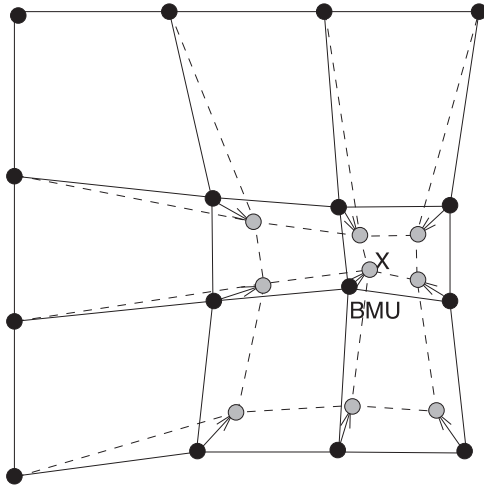
Fig. 2 – Updating the best matching unit (BMU) and its neighbours towards the input sample marked with *x*. The solid and dashed lines correspond to the situation before and after updating, respectively.

is chosen randomly and the distances between it and all the weight vectors of the SOM are calculated using some distance measure. The neuron whose weight vector is closest to the input vector *x* is called the best-matching unit (BMU), denoted here by *c*:

$$\|x - m_c\| = \min_i \{\|x - m_i\|\} \tag{1}$$

where $\| \quad \|$ is the distance measure, typically Euclidean distance.

After finding the BMU, the weight vectors of the SOM are updated so that the BMU is moved closer to the input vector in the input space. The topological neighbours of the BMU are treated similarly. This adaptation procedure stretches the BMU and its topological neighbours towards the sample vector as shown in Fig. 2.

The SOM update rule for the weight vector of unit *i* is:

$$m_i(t+1) = m_i(t) + \alpha(t)h_{ci}(t)[x(t) - m_i(t)], \tag{2}$$

where *t* denotes time. The *x*(*t*) is an input vector randomly drawn from the input data set at time *t*, $h_{ci}(t)$ the neighbourhood kernel around the winner unit *c* and $\alpha(t)$ the learning rate at time *t*.

The neighbourhood kernel is a non-increasing function of time and of the distance of unit *i* from the winner unit *c*. It defines the region of influence that the input sample has in the SOM. The training is usually performed in two phases. In the first phase, relatively large initial learning rate and neighbourhood radius are used. In the second phase, both learning rate and the neighbourhood radius are small from the beginning. This procedure corresponds to start tuning the SOM approximately to the same space as the input data an then fine-tuning the map in the second phase.

Once the map training is finished, the visualization of the two-dimensional map named "components plane"

provides qualitative information about how the input variables are related to each other for the data set used to train the map.

2.2. Supervised SOM

In the present paper, it is decided to apply a supervised SOM because a supervised problem is faced, that is, each pattern is associated with a class, so it is essential to obtain results according to that information. Therefore, it is interesting to use a supervised SOM that provides information about the class in the training.

The supervised SOM algorithm creates, initializes and trains a supervised SOM. It constructs the training data by adding *M* (number of classes) columns to the original data based on the class information. Therefore, the dimension of vectors after the process is $N+M$ (dimension of the input vectors +number of different classes). In each input vector, one of the new components has value '1' (if the input vector belongs to the class corresponding with the new component), and others '0' (if it does not belong to this class). After this, the classical approach presented in Section 2.1 is carried out. Then, the class of each map unit is determined by taking the maximum over these added components, and a label is given accordingly. Finally, the extra components are removed. In this work, instead of labelling a map with the labels provided by the algorithm, a colored "Hits map" is presented. The next section explains in detail this kind of map.

2.3. Hits map

A "Hits map" represents the response of the given data on self-organising maps. Traditionally the response is shown on the map by showing the BMU [35], so the map presented has the same size that the components plane of the SOM. "Hits map" are markers showing how many times each map unit, or neuron, was the BMU for each input register so that the distribution of the best matching units for a given data set is represented. Fig. 3 shows an example of a conventional "Hits map", where each neuron is represented by an hexagon on the map grid. The colored area inside each hexagon is proportional to the number of input patterns which are more similar to this neuron. This gives a quantitative idea of the patients belonging to each neuron. Moreover, multiple "hits" can be drawn in different colors. This makes possible to compare the different patterns associated to each class by the distribution of their "hits" on the map. As we will see in Section 4, these maps provide more information than those obtained by simple labelling.

3. Data set

This section details the characteristics of the dataset used in this study and the parameteres extracted from the ECG signals.
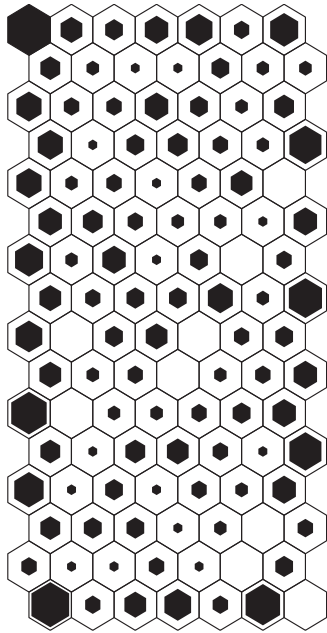
Fig. 3 – Example of a conventional "Hits map", where each neuron is represented by an hexagon on the map grid. The colored area inside each hexagon is proportional to the number of input patterns which are more similar to this neuron.

3.1.   ECG data

ECG signals were collected from the AHA Arrhythmia Database[1] (8200 series) and the MIT-BIH Malignant Ventricular Arrhythmia database[2] where a single ECG channel is used. A total of 29 patient recordings were analysed, each containing an average of 30 min of continuous ECG, from which approximately 100 min corresponded to VF. For each record, non-overlapping 128 sample length segments sampled at 125 Hz were used, giving a 1.024 s of continuous time window segment for the analysis. In total 57,908 observations were obtained. Before parameter calculation, a general signal pre-processing was done, firstly subtracting the mean ECG signal value, and secondly, low-pass filtering with cutoff frequency of 40 Hz to remove the electrical network interference and other high frequency components not relevant for the analysis. Fibrillatory rhythms are characterized by an absence of regularity in the ECG signal due to the creation of multiple independent re-entry activation circuits in the heart tissue, avoiding the correct transmission of the sinus activation pulse. This disorganised contraction of the ventricle fails to effectively eject blood from the ventricle, provoking a heart collapse. Figs. 4 and 5 show the time, frequency and time–frequency results for an analysed ECG window segment in a normal sinus and a fibrillatory rhythm, respectively.

---

[1] http://ecri.org (American Heart Association ECG Database).
[2] http://physionet.org.

3.2.   Time–frequency domain parameters

Each window segment was processed to obtain a set of temporal (t), spectral (f) and time–frequency (tf) domain parameters. Before parameter calculation in the tf distribution, a denoising is done, consisting on removing all components less than 10% of the maximum spectral density value. These low value components are formed by noise or small interference terms (time–frequency distributions generate the so-called interference terms) [45] and they do not add useful information.

Parameters are obtained from the Pseudo Wigner-Ville (PWV) time–frequency distribution as previously described in [21,32], only two out of twenty-seven parameters come from the temporal signal, the rest are obtained from the PWV distribution.

In order to characterize and differentiate fibrillatory episodes from other cardiac rhythms, two spectral bands of interest were defined [14] in the tf domain. Since most of the energy components of fibrillatory episodes reside in the low frequencies band, we defined a low frequency band (2–14 Hz) called BALO. A high frequency band (BAHI, 14–28 Hz) was also considered, mainly containing energy components for non-VF rhythms. Based on the PWV distribution and the defined frequency bands, a number of temporal, spectral, and time–frequency parameters have been obtained (see Table 1). The chosen parameters provide different information about power spectral distribution along time, duration of significant frequency bands (those containing sinus or fibrillatory rhythms), and in general, all information leading to different measures from ECG rhythms that could provide useful information depending on the patient's pathology. The selection of relevant time–frequency parameters is very important for a sucessful further analysis and was carefully chosen after data analysis. A detailed description of the parameters can be found in [32,46,47].

Parameterization of ECG signal segments results in an input data set to the SOM consisting of $L = 57$, 908 observations each containing 27 features. Each observation was labeled into four groups according to different rhythms, which appeared with different prior probabilities: HP ($p_1 = 40.25\%$), for healthy patients; VT ($p_2 = 8.84\%$), for ventricular tachycardia (VT) including their variants (regular VT, polymorphic VT or "torsade de pointes"); VF ($p_3 = 10.66\%$), for VF signal and flutter; and AHR ($p_4 = 40.25\%$), comprising the rest of cardiac rhythms.

4.   Results

This section presents the results obtained with the data set put forward in Section 3. In order to explore different possibilities and results, three analysis were performed. This section is divided into three subsections which detail the different experiments carried out and their results.

The first problem found in this work is the large number of variables as discussed in Section 3, some of which may be redundant. Therefore, a feature selection must be carried out. In a previous work [46], it is proposed the use of nonparametric bootstrap resampling technique using the same type of data as in the present work to provide a criterion for feature
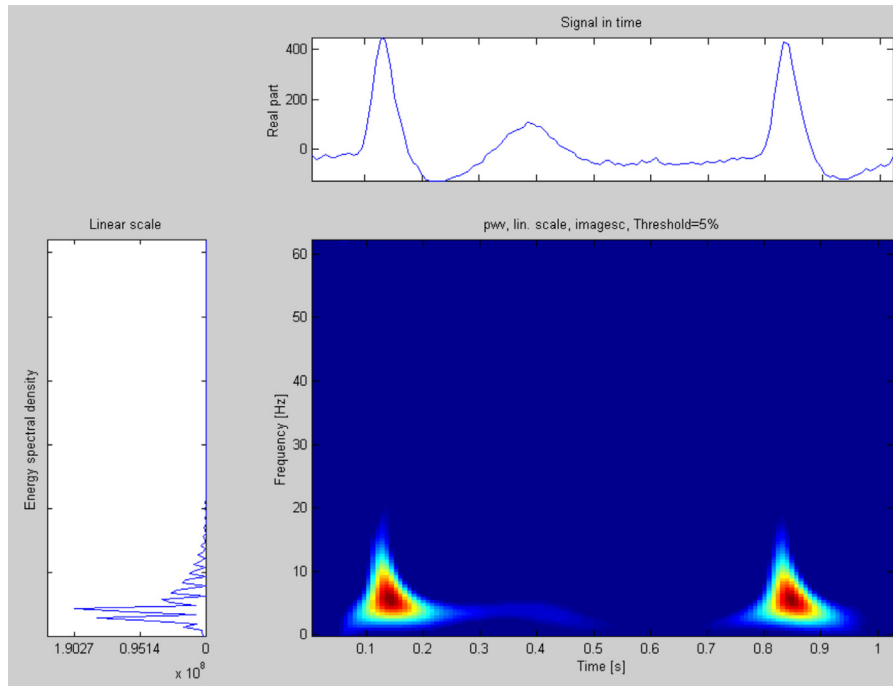
Fig. 4 – Normal sinus rhythm in the surface ECG. Temporal signal (top) and its associated frequency (left) and PWV time–frequency representations.

selection (11 features were selected). After selecting the variables pointed out in [46], the training of several SOM was carried out. For the training, different options of the tuning parameters of the SOM algorithm were tested, combining all the possibilities (Weight Initialization, Neighbourhood Function and Type of Training). Moreover, the random initialization was fulfilled 100 times for each combination of parameters. Regarding the size of the map, the total training time, the learning rate and the neighbourhood radius, the default number of these parameters that SOM toolbox
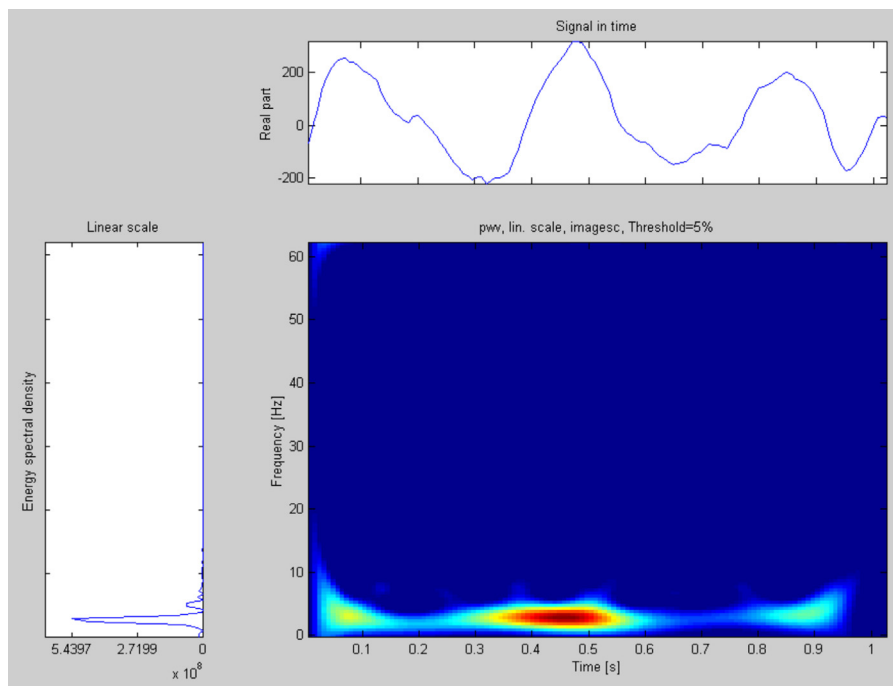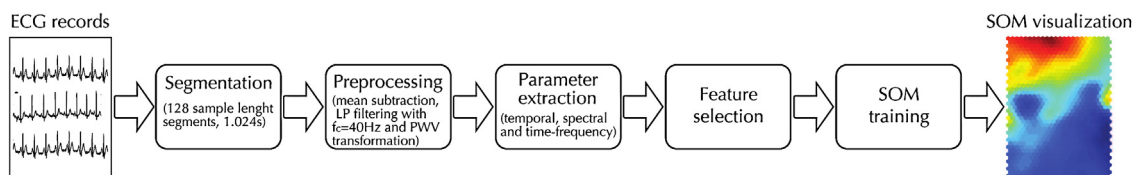

Fig. 5 – Ventricular fibrillation rhythm in the surface ECG. Temporal signal (top) and its associated frequency (left) and PWV time–frequency representations.

Table 1 – Obtained time–frequency parameters (mean ± sd), where the "t" and "tf" in the "Domain" column refers to temporal and time–frequency domains.

#	Variable	Domain	HP	AHR	VT	VF
1	VR	t	$(8.2 \pm 6.7) \cdot 10^{+0}$	$(6.0 \pm 5.0) \cdot 10^{+0}$	$(1.6 \pm 3.4) \cdot 10^{+0}$	$(1.5 \pm 1.1) \cdot 10^{+0}$
2	ratiovar	t	$(1.6 \pm 0.5) \cdot 10^{+0}$	$(1.8 \pm 0.5) \cdot 10^{+0}$	$(2.5 \pm 0.6) \cdot 10^{+0}$	$(2.7 \pm 0.4) \cdot 10^{+0}$
3	pmxfrec	f	$(5.5 \pm 3.2) \cdot 10^{+0}$	$(4.0 \pm 2.5) \cdot 10^{+0}$	$(2.8 \pm 2.0) \cdot 10^{+0}$	$(2.6 \pm 1.2) \cdot 10^{+0}$
4	maximfrec	f	$(2.2 \pm 0.8) \cdot 10^{+1}$	$(2.0 \pm 0.7) \cdot 10^{+1}$	$(1.5 \pm 0.8) \cdot 10^{+1}$	$(1.4 \pm 0.5) \cdot 10^{+1}$
5	minimfrec	f	$(7.3 \pm 4.9) \cdot 10^{-1}$	$(6.3 \pm 3.8) \cdot 10^{-1}$	$(6.4 \pm 3.5) \cdot 10^{-1}$	$(6.9 \pm 3.6) \cdot 10^{-1}$
6	tsnz	tf	$(1.1 \pm 0.6) \cdot 10^{+3}$	$(1.1 \pm 0.6) \cdot 10^{+3}$	$(1.6 \pm 0.5) \cdot 10^{+3}$	$(1.5 \pm 0.4) \cdot 10^{+3}$
7	tsnzl	f	$(6.4 \pm 3.1) \cdot 10^{+2}$	$(6.8 \pm 3.0) \cdot 10^{+2}$	$(1.2 \pm 3.1) \cdot 10^{+2}$	$(1.2 \pm 3.0) \cdot 10^{+2}$
8	qtl	f	$(0.6 \pm 1.0) \cdot 10^{-1}$	$(6.5 \pm 1.0) \cdot 10^{-1}$	$(7.7 \pm 1.1) \cdot 10^{-1}$	$(8.1 \pm 1.1) \cdot 10^{-1}$
9	tsnzh	f	$(2.0 \pm 2.3) \cdot 10^{+2}$	$(1.8 \pm 2.2) \cdot 10^{+2}$	$(1.5 \pm 2.1) \cdot 10^{+2}$	$(1.2 \pm 1.7) \cdot 10^{+2}$
10	qth	f	$(1.8 \pm 1.0) \cdot 10^{-1}$	$(1.5 \pm 0.9) \cdot 10^{-1}$	$(0.8 \pm 0.9) \cdot 10^{-1}$	$(0.6 \pm 0.7) \cdot 10^{-1}$
11	mdl8	t	$(9.1 \pm 4.1) \cdot 10^{+1}$	$(8.6 \pm 3.8) \cdot 10^{+1}$	$(6.8 \pm 3.5) \cdot 10^{+1}$	$(6.1 \pm 2.4) \cdot 10^{+1}$
12	vdl8	t	$(9.7 \pm 4.2) \cdot 10^{+1}$	$(8.7 \pm 3.8) \cdot 10^{+1}$	$(4.9 \pm 2.8) \cdot 10^{+1}$	$(4.5 \pm 2.0) \cdot 10^{+1}$
13	te	tf	$(0.6 \pm 1.0) \cdot 10^{+9}$	$(0.2 \pm 5.1) \cdot 10^{+10}$	$(0.1 \pm 2.0) \cdot 10^{+11}$	$(1.2 \pm 1.9) \cdot 10^{+9}$
14	tel	f	$(4.8 \pm 7.0) \cdot 10^{+8}$	$(0.1 \pm 2.6) \cdot 10^{+10}$	$(0.7 \pm 9.3) \cdot 10^{+10}$	$(1.1 \pm 1.5) \cdot 10^{+9}$
15	qtel	f	$(7.1 \pm 1.1) \cdot 10^{-1}$	$(7.3 \pm 1.1) \cdot 10^{-1}$	$(8.3 \pm 1.0) \cdot 10^{-1}$	$(0.9 \pm 1.0) \cdot 10^{-1}$
16	teh	f	$(0.8 \pm 1.2) \cdot 10^{+8}$	$(0.4 \pm 18.) \cdot 10^{+9}$	$(0.3 \pm 7.3) \cdot 10^{+10}$	$(0.3 \pm 1.2) \cdot 10^{+8}$
17	qteh	f	$(1.7 \pm 1.2) \cdot 10^{-1}$	$(1.1 \pm 0.8) \cdot 10^{-1}$	$(0.5 \pm 0.7) \cdot 10^{-1}$	$(0.3 \pm 0.5) \cdot 10^{-1}$
18	ct8	t	$(3.7 \pm 1.6) \cdot 10^{+0}$	$(3.9 \pm 1.5) \cdot 10^{+0}$	$(6.3 \pm 1.3) \cdot 10^{+0}$	$(6.2 \pm 1.3) \cdot 10^{+0}$
19	tmy	tf	$(1.5 \pm 0.7) \cdot 10^{+2}$	$(1.5 \pm 0.6) \cdot 10^{+2}$	$(2.9 \pm 1.2) \cdot 10^{+2}$	$(2.7 \pm 1.3) \cdot 10^{+3}$
20	curve	f	$(1.4 \pm 1.7) \cdot 10^{-1}$	$(1.7 \pm 1.7) \cdot 10^{-1}$	$(-1.0 \pm 2.8) \cdot 10^{-1}$	$(-1.8 \pm 3.0) \cdot 10^{-1}$
21	nareas	tf	$(1.4 \pm 0.7) \cdot 10^{+0}$	$(1.4 \pm 0.9) \cdot 10^{+0}$	$(2.0 \pm 0.9) \cdot 10^{+0}$	$(1.8 \pm 0.8) \cdot 10^{+0}$
22	lfrec	f	$(9.9 \pm 4.5) \cdot 10^{+0}$	$(8.0 \pm 3.1) \cdot 10^{+0}$	$(6.1 \pm 4.2) \cdot 10^{+0}$	$(5.0 \pm 1.5) \cdot 10^{+0}$
23	maxfrec	f	$(1.3 \pm 0.5) \cdot 10^{+1}$	$(1.0 \pm 0.4) \cdot 10^{+1}$	$(0.8 \pm 0.5) \cdot 10^{+1}$	$(0.7 \pm 0.2) \cdot 10^{+1}$
24	minfrec	f	$(2.6 \pm 1.6) \cdot 10^{+0}$	$(2.2 \pm 1.4) \cdot 10^{+0}$	$(1.9 \pm 0.9) \cdot 10^{+0}$	$(2.0 \pm 0.8) \cdot 10^{+0}$
25	ltmp	t	$(1.5 \pm 1.1) \cdot 10^{+1}$	$(1.7 \pm 1.3) \cdot 10^{+1}$	$(3.4 \pm 2.1) \cdot 10^{+1}$	$(3.5 \pm 2.2) \cdot 10^{+1}$
26	dispersion	tf	$(2.1 \pm 4.6) \cdot 10^{+0}$	$(1.9 \pm 4.6) \cdot 10^{+0}$	$(5.9 \pm 7.7) \cdot 10^{+0}$	$(5.8 \pm 7.8) \cdot 10^{+0}$
27	area	tf	$(1.3 \pm 1.1) \cdot 10^{+2}$	$(1.3 \pm 1.0) \cdot 10^{+2}$	$(1.9 \pm 1.4) \cdot 10^{+2}$	$(1.7 \pm 1.1) \cdot 10^{+2}$

Fig. 6 – Methodology carried out in this study.

documentation considers the most appropriate was selected[3]. These values are $5\sqrt{n}$, where n is the number of training samples for the number or neurons. For the total training time (or, the number of samples presented to the SOM) the default value is 10 times the number of map units. Learning rate begins from 0.5 in the first phase, and from 0.05 in the second phase. Neighbourhood radius starts from max(map size)/4 and goes down to one fourth of that (unless this would be less than 1). On second phase, neighbourhood radius starts from where it stopped in first phase, and goes down to 1. The length of second phase is 4 times that of the first phase.

Finally, it was selected the SOM that showed the minimum topographic error [48], which measures the topology preservation between the original space and the final space. To summarize, Fig. 6 shows the methodology carried out in this study. The first step after recording the ECG is the segmentation of the signals, giving a 1.024 s of continuous time window segment for the analysis. In total 57,908 observations were obtained. After segmentation, a pre-processing of each observation is done, which consists of mean subtraction

and low-pass filtering. Afterwards, the parameter extraction is done by processing each window segment to obtain a set of temporal (t), spectral (f) and time–frequency (tf) domain parameters. After that, a feature selection is carried out, obtaining the final data set to train the SOM. This set consists of a matrix with 57,908 observations (rows) and 11 variables (columns). The last steps are the SOM training, and visualization by means of the components plane (before that it will be represented the hits map in order to compare the different patterns associated to each class by the distribution of their "hits" on the map).

4.1. Supervised SOM training

In this section the four pathology groups (VF, VT, HP and AHR) are included separately in the training. Once the map training is finished, the visualization of the two-dimensional map provides qualitative information about the input variables relationships for the data set used to train the map. Before visualizing the SOM components map, the "Hits map" is represented in order to get spatial information about the classes in the map (Fig. 7), that is, where each patient (corresponding to each class) is placed in the map.
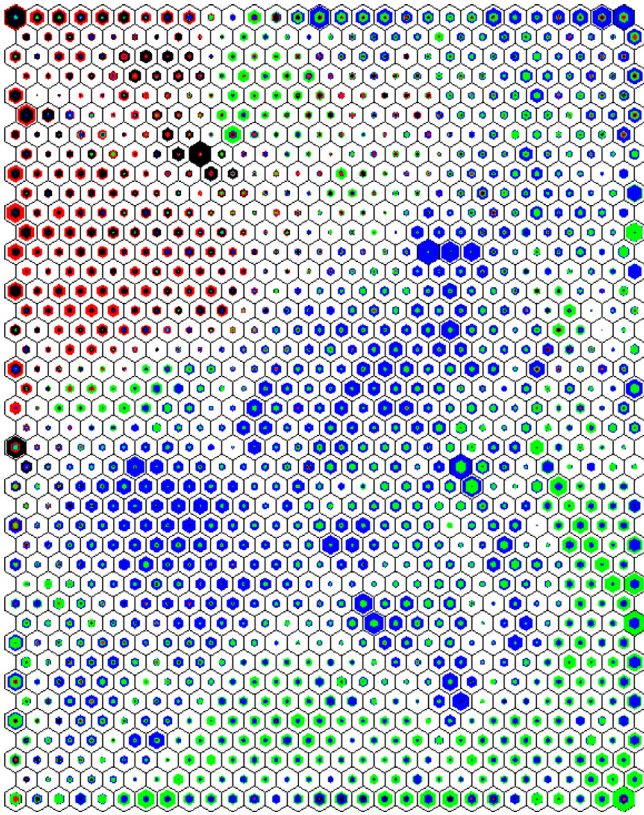
---

[3] http://www.cis.hut.fi/somtoolbox/documentation/somalg.shtml

Fig. 7 – "Hits map" obtained from the training with four groups of patients. VF is represented in red, VT in black, HP in green and AHR in blue. (For interpretation of the references to color in this figure legend, the reader is referred to the web version of this article.)

The "Hits map" shows pathology groups with different colors (corresponding to each class) instead of directly labelling the map with the labels provided by the algorithm, as mentioned previously. This map provides more information than simply labelling because in each neuron (each hexagon on the map grid) we have information about all classes presented in a neuron instead of representing only the predominant class by a color.

Fig. 7 shows that the classes labelled as VF (patients who suffer from ventricular fibrillation) and VT (patients who suffer from ventricular tachycardia) are very similar since they are completely overlapped. This is due to the fact that, in many cases, VT is an early stage of VF and thus, the pathologies can be considered as very similar in case of pathology profiling although the clinical recovering therapy for VT and VF is not the same. However, VT could be considered as the beginning of VF and thus, it was decided to join both classes in one to be able to extract knowledge, and to visually identify which variables are important to obtain differences between healthy patients and patients with ventricular fibrillation or ventricular tachycardia. For this reason another experiment was evaluated taking into account only VF and VT. However, both classes were overlapped even in this analysis. Due to the experiment did not provide relevant information it is not included in this paper.

4.2. Supervised SOM training merging VF and VT classes

In this section, the results corresponding to the map using supervised training for three groups of patients are presented. These three groups correspond to: patients with ventricular fibrillation or ventricular tachycardia (VFVT as the merging of VF and VT classes), healthy patients (HP) and anomalous heart rates and noise (AHR).

Fig. 8 shows the "Hits map" obtained from the training with these three groups of patients. It shows that AHR class (which included both anomalous heart rates and noise) spreads over the HP class (represented in green), which is not critical. That is, it would be a problem that other heart rates or noise would be overlapped with ventricular fibrillation or ventricular tachycardia because, in this case, it would not be possible to profile the diseases of interest (VF and VT). In this work, it is of great interest profiling patients with ventricular fibrillation or ventricular tachycardia pathology versus healthy patients using visual information of the variables in order to observe differences between both groups. Therefore, the AHR class is not determinative to profile healthy patients versus those suffering VF or VT. Moreover, to carry out the study in ideal conditions (without taking into account noise, only to obtain visual information between the differences in healthy and non-healthy patients) is of interest in order to profile patients
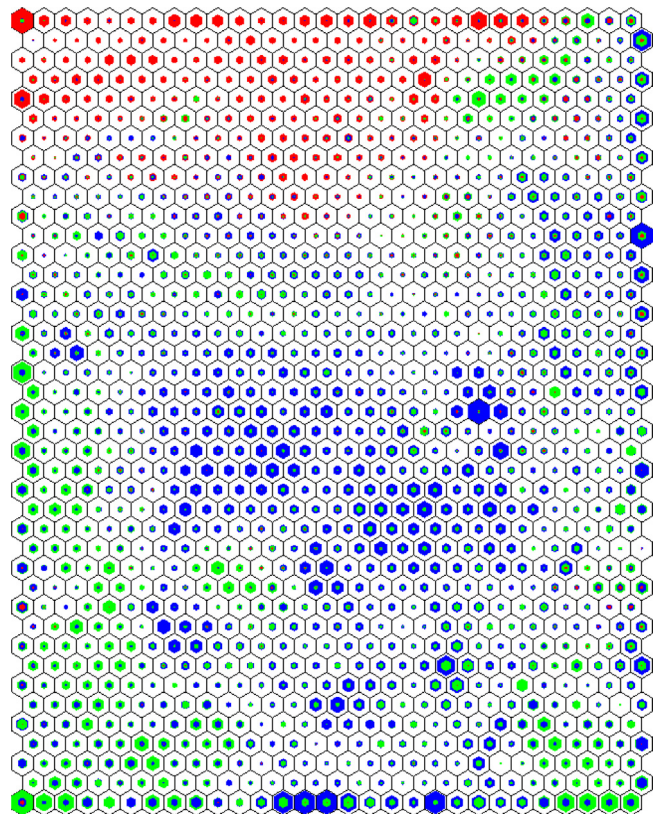

Fig. 8 – "Hits map" obtained from the training with three groups of patients. VFVT is represented in red, HP in green and AHR in blue. (For interpretation of the references to color in this figure legend, the reader is referred to the web version of this article.)

suffering from VF and VT versus healthy patients. Due to these facts, further analysis is done drawing the patterns belonging to this class.

4.3.   Supervised SOM training merging VF and VT classes without AHR class

This section presents the results corresponding to the map using supervised training with two groups of patients (ideal condition), as mentioned previously. These two groups correspond to: patients who suffer ventricular fibrillation or ventricular tachycardia (VFVT) and healthy patients (HP).

Fig. 9 represents "Hits map" obtained from the training with the two above-mentioned groups of patients. Fig. 9 shows that HP class (represented in green) and VFVT class (represented in red) are clearly distinguishable. In general terms, the patients who suffer from some ventricular fibrillation or ventricular tachycardia (VFVT) are located at the bottom of the map, whereas the healthy patients (HP) are located at the top of the map. Therefore, there exist differences in the behavioural profile of each group of patients. To analyse the profiles of
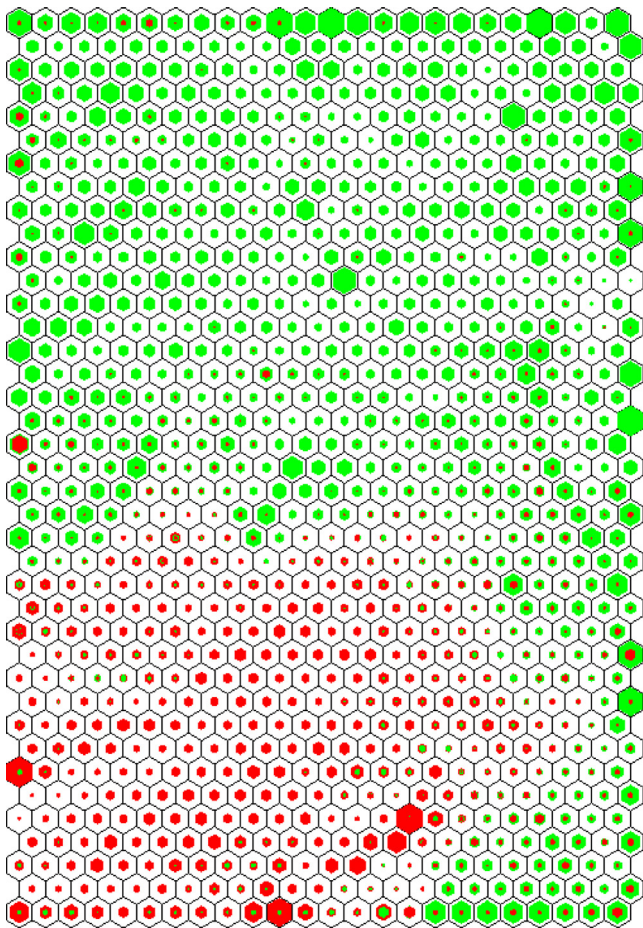

Fig. 9 – "Hits map" obtained from the training with two groups of patients. VFVT is represented in red, and HP in green. (For interpretation of the references to color in this figure legend, the reader is referred to the web version of this article.)

each group of patients, the components plane obtained after training the SOM (Fig. 10) must be examined.

Fig. 10 shows that there are three important variables when differentiating between healthy patients and those suffering from ventricular fibrillation or ventricular tachycardia. These variables are qtel, ct8 and curve, described as:

- qtel: percentage of the total spectral density contained in the BALO band. In case of a VFVT, the main spectral density is located in the BALO band.
- ct8: the time axis of the PWV distribution is divided into eight window subsegments. Then, for every subsegment, the energy in the BALO band is measured. The *ct8* corresponds to the number of subsegments that contain at least half of the spectral density if the total density of the band would be equally distributed along the time axis.
- curve: a vector containing the number of non-zero terms at every frequency bin of spectral resolution in the BALO and BAHI bands is computed and the curvature of the parabolic approximation of the vector is obtained. This value gives information about distribution of frequency terms along time. In case of HP, frequency distribution is not regular due to the QRS existence (high frequency terms are dominant) and the curvature is higher, which is contrary to the existence of an VFVT rhythm where frequency distribution is spread along all analysed frequencies and the parabolic approximation curvature is lower.

This is due to the fact that the values of these variables undergo significant changes in the area where the patients suffering from ventricular fibrillation or ventricular tachycardia are located (bottom of the map) with respect to the area in which healthy patients are situated (top of the map). In case of patients who suffer from VF or VT the qtel and ct8 variables take higher values (see areas with frame in Fig. 10), whereas the curve variable takes lower values. This is contrary to healthy patients, showing lower values in the rest of the map to the variables qtel and ct8 (except in the upper right area of qtel map) and higher values in the rest of map for the curve variable. The importance of these variables is due to the fact that VF and VT pathologies are very irregular both in time and frequency. Concerning qtel, the non-existence of a front wave in the heart avoids the blood being pumped from the heart (QRS absence) in case of VF and all spectral density components are mainly located in the BALO band. A similar reason arises in case of ct8 due to the fact that distribution of density components along time is more regular in VF than in case of ECG existence (healthy patients) where specific time instants concentrate most of the spectral density. Thus, eventhough the variables use both domains, qtel and ct8 provide relevant information related to frequency domain and time domain respectively. Finally, curve provides a combined information for both domains, showing that, due to special characteristics of VF, an adequate discrimination algorithm requires the usage of different domains.

Other training results obtained in Sections 4.1 and 4.2 show the same behaviour with regard to the qtel, ct8 and curve variables, being the most important to separate between patients who suffer from VF or VT and healthy patients.
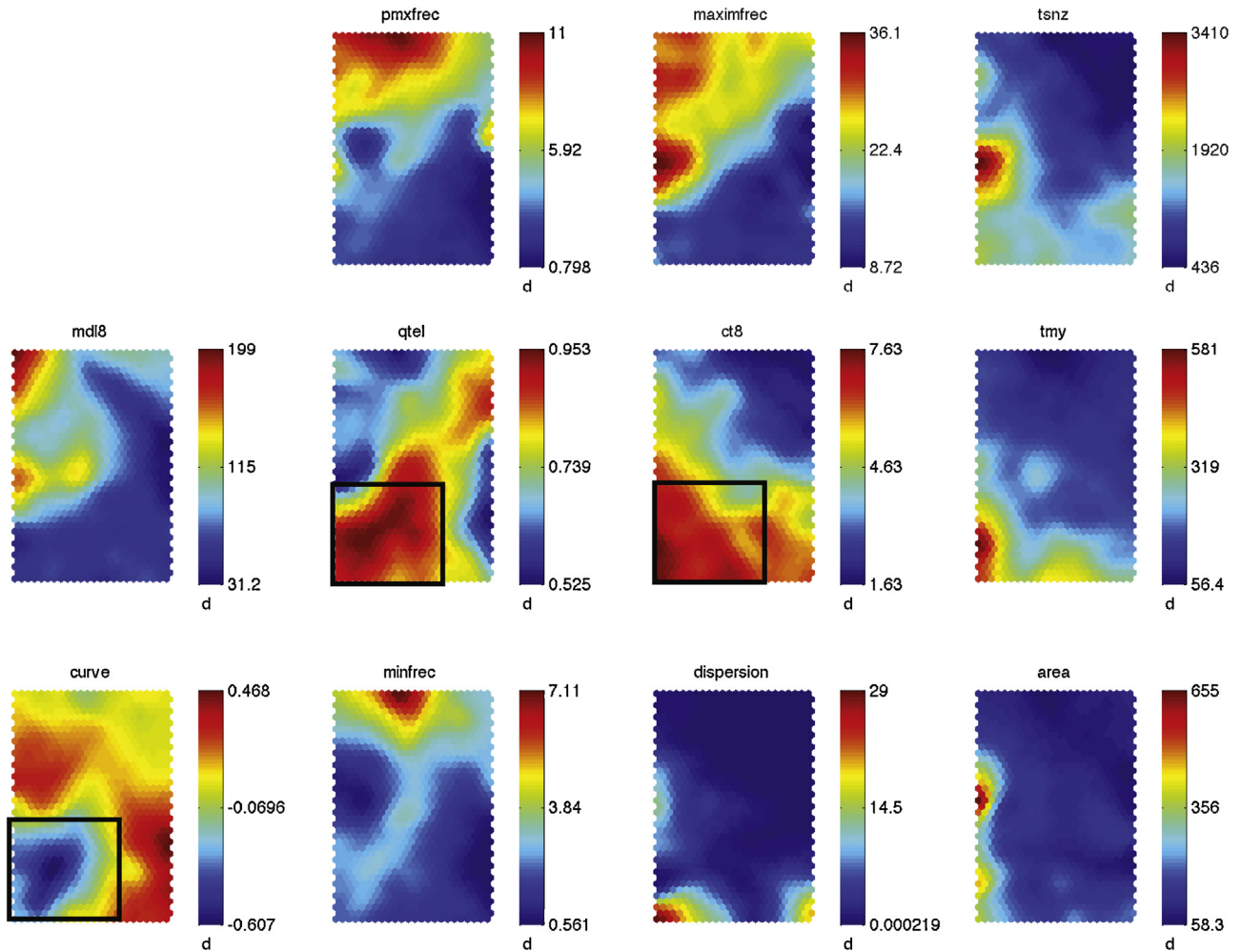
Fig. 10 – "Components plane" obtained from the training with two groups of patients (VFVT and HP).

5.   Conclusions

This paper proposes the use of a supervised self-organising map (SOM) to extract qualitative information about how the input variables are related to each other about four groups of patients: VF, VT, HP and AHR. In order to address the problem, three different trainings were carried out. Firstly, a supervised training considering all classes. It was noted that VF and VT classes were very similar (they were placed in the same location of the map) since, in many cases, VT is an early stage of VF and thus, the pathologies can be considered as very similar in case of pathology profiling. For this reason, it was decided to merge these two classes since it does not entail an extremely relevant fact for visual analysis of the problem.

Finally, after noting that the AHR class did not provide relevant information to the problem, and with the aim of carrying out a final study only with the classes corresponding to patients who suffer ventricular fibrillation or ventricular tachycardia (VFVT) and healthy patients (HP), it was decided to draw the patterns corresponding to this class. Thus, the analysis was targeted to visual distinction between healthy patients and those suffering from ventricular fibrillation or ventricular tachycardia using the components map obtained

after training the SOM. It was observed a clear visual separation, resulting that the most relevant variables were qtel, ct8 and curve. This analysis also showed that it was possible to perform a profile of patients suffering from ventricular fibrillation or ventricular tachycardia and other corresponding to healthy patients.

REFERENCES

[1] G.K. Moe, J.A. Abildskov, J. Han, Factors responsible for the initiation and maintenance of ventricular fibrillation., in: B. Surawicz, E. Pellegrino (Eds.), Sudden Cardiac Death, Grune and Stratton, New York, 1964.

[2] C.S. Beck, W.H. Pritchard, W. Giles, G. Mensah, Ventricular fibrillation of long duration abolished by electric shock, Journal of the American Medical Association 135 (1947) 985–986.

[3] R.W. Yakaitis, G.A. Ewy, C.W. Otto, Infuence of time and therapy on ventricular fibrillation in dogs, Critical Care Medicine 8 (3) (1980) 157–163.

[4] A. Capucci, D. Aschieri, M. Piepoli, A. Rosi, M. Arvedi, G. Villani, Early defibrillation through first responders triples survivals rates from out of hospital cardiac arrest in an Italian community, European Heart Journal 22 (2001) 242.

[5] R. White, B. Asplin, T. Bugliosi, D. Hankins, High discharge survival rate after out-of-hospital ventricular fibrillation with rapid defibrillation by police and paramedics, Annals of Emergency Medicine 28 (5) (1996) 480–485.

[6] S.C. Faddy, Reconfirmation algorithms should be standard of care in automated external defibrillators, Resuscitation 68 (3) (2006) 409–415.

[7] S. Chen, N.V.T. NV, M.M. Mower, Ventricular fibrillation detection by a regression test on the autocorrelation function, Medical & Biological Engineering & Computing 25 (3) (1987) 241–249.

[8] R.H. Clayton, A. Murray, R.W. Campbell, Comparison of four techniques for recognition of ventricular fibrillation from the surface ECG, Medical & Biological Engineering & Computing 31 (2) (1993) 111–117.

[9] S.W. Chen, P.M. Clarkson, Q. Fan, A robust sequential detection algorithm for cardiac arrhythmia classification, IEEE Transactions on Biomedical Engineering 43 (11) (1996) 1120–1125.

[10] X.S. Zhang, Y.S. Zhu, N.V. Thakor, Z.Z. Wang, Detecting ventricular tachycardia and fibrillation by complexity measure, IEEE Transactions on Biomedical Engineering 46 (5) (1999) 548–555.

[11] J.M. Davidenko, A.V. Pertsov, R. Salomonsz, W. Baxter, J. Jalife, Stationary and drifting spiral waves of excitation in isolated cardiac muscle, Nature 355 (6358) (1992) 349–351.

[12] R.H. Clayton, A. Murray, R.W. Campbell, Evidence for electrical organization during ventricular fibrillation in the human heart, Journal of Cardiovascular Electrophysiology 6 (8) (1995) 616–624.

[13] J. Jalife, R.A. Gray, G.E. Morley, J.M. Davidenko, Evidence for electrical organization during ventricular fibrillation in the human heart, Chaos 8 (1) (1998) 79–93.

[14] J.N. Herschleb, R.M. Heethaar, I.V. de Tweel, A.N.E. Zimmerman, F.L. Meijler, Signal analysis of ventricular fibrillation, IEEE Computers in Cardiology (1979) 49–54.

[15] A. Murray, R.W.F. Campbell, D.G. Julian, Characteristics of the ventricular fibrillation waveform, IEEE Computers in Cardiology (1985) 275–278.

[16] M.E. Nygards, J. Hulting, Recognition of ventricular fibrillation utilizing the power spectrum of the ECG, IEEE Computers in Cardiology (1978) 393–397.

[17] S. Barro, R. Ruiz, D. Cabello, J. Mira, Algorithmic sequential decision making in the frequency domain for life threatening centricular arrhythmias and aimitative artifacts: a diagnostic system, Journal of Biomedical Engineering 11 (4) (1989) 320–328.

[18] F.M. Nolle, R.W. Bowser, F.K. Badura, J.M. Catlett, R.R. Gudapati, T.T. Hee, A.N. Moos, M.H. Sketch Sr., Evaluation of frequency-domain algorithm to detect ventricular fibrillation in the surface electrocardiogram, IEEE Computers in Cardiology (1988) 337–340.

[19] V.X. Afonso, W.J. Tompkins, Detecting ventricular fibrillation, IEEE Engineering in Medicine & Biology 14 (2) (1995) 152–159.

[20] R.H. Clayton, A. Murray, Comparison of techniques for time–frequency analysis of the ECG during human ventricular fibrillation, IEEE Proceedings on Science and Measurements Technology 145 (1998) 301–306.

[21] A. Rosado, A. Serrano, M. Martínez, E. Soria, J. Calpe, M. Bataller, Detailed study of time–frequency parameters for ventricular fibrillation detection, in: ESEM Europen Society for Engineering and Medicine, 1999, pp. 379–380.

[22] A. Amann, R. Tratnig, K. Unterkofler, Detecting ventricular fibrillation by time-delay methods, IEEE Transactions on Biomedical Engineering 54 (1) (2007) 174–177.

[23] B. Bai, Y. Wang, Ventricular fibrillation detection based on empirical mode decomposition., Bioinformatics and Biomedical Engineering, (iCBBE) 2011 5th International Conference on (2011) 1–4.

[24] Y. Li, J. Bisera, M. Weil, W. Tang, An algorithm used for ventricular fibrillation detection without interrupting chest compression, IEEE Transactions on Biomedical Engineering 59 (1) (2012) 78–86.

[25] C. Zhang, J. Zhao, J. Tian, F. Li, H. Jia, Support vector machine for arrhythmia discrimination with tci feature selection, in: Communication Software and Networks (ICCSN), 2011 IEEE 3rd International Conference on, 2011, pp. 111–115.

[26] A. Amann, R. Tratnig, K. Unterkofler, Reliability of old and new ventricular fibrillation detection algorithms for automated external defibrillators, BioMedical Engineering Online 4 (60) (2005 October).

[27] R.H. Clayton, A. Murray, R.W. Campbell, Recognition of ventricular fibrillation using neural networks, Medical & Biological Engineering & Computing 32 (2) (1994) 217–220.

[28] A. Neurauter, T. Eftestol, J. Kramer-Johansen, B.S. Abella, K. Sunde, V. Wenzel, K.H. Lindner, J. Eilevstjonn, H. Myklebust, P.A. Steen, H.-U. Strohmenger, Prediction of countershock success using single features from multiple ventricular fibrillation frequency bands and feature combinations using neural networks, Resuscitation 73 (2) (2007) 253–263.

[29] J. Pardey, Detection of ventricular fibrillation by sequential hypothesis testing of binary sequences, IEEE Computers in Cardiology (2007) 573–576.

[30] I. Jekova, P. Mitev, Detection of ventricular fibrillation and tachycardia from the surface ecg by a set of parameters acquired from four methods, Physiological Measurement 23 (4) (2002 November) 629–634.

[31] E.D. Übeyli, Usage of eigenvector methods in implementation of automated diagnostic systems for ecg beats, Digital Signal Processing 18 (1) (2008) 33–48.

[32] A. Rosado-Mu noz, G. Camps-Valls, J. Guerrero-Martínez, J.V. Francés-Villora, J. Mu noz-Marí, A.J. Serrano-López, Enhancing feature extraction for VF detection using data mining techniques, IEEE Computers in Cardiology 29 (2002) 209–212, http://dx.doi.org/10.1109/CIC.2002.1166744.

[33] T. Kohonen, Self-organization and associative memory, third ed., Springer-Verlag New York, Inc, New York, NY, USA, 1989.

[34] T. Kohonen, Self-organized formation of topologically correct feature maps, Biological Cybernetics 43 (1982) 59–69.

[35] T. Kohonen, Self-Organizing Maps, third ed., Springer Berlin Heidelberg, 2000.

[36] S. Haykin, Neural Networks and Learning Machines., third ed., Prentice Hall, 2009.

[37] G.J. Deboeck, T.K. Kohonen (Eds.), Visual Explorations in Finance., first ed., Springer-Verlag New York, Inc, Secaucus, NJ, USA, 1998.

[38] Y. Alakhdar, J.M. Martínez-Martínez, J. Guimerà-Tomás, P. Escandell- Montero, J. Benítez, E. Soria-Olivas, Visual data mining in physiotherapy using self-organazing maps: a new approximation to the data analysis, in: R. Magdalena, E. Soria, J. Guerrero, J. Gómez (Eds.), Medical Application of Intelligent Data Analysis: Research Advancements, IGI Global, 2012, pp. 186–193, Ch. 12.

[39] T. Kohonen, E. Oja, O. Simula, A. Visa, J. Kangas, Engineering applications of the self-organizing map, Proceedings of the IEEE 4 (10) (1996) 1358–1384.

[40] I. Díaz, A.A. Cuadrado, A.B. Diez, M. Domínguez, J.J. Fuertes, M.A. Prada, Supervision of industrial processes using self organizing maps, in: R. Magdalena-Benedito, M. Martínez-Sober, J.M. Martínez-Martínez, P. Escandell-Montero, J. Vila-Francés (Eds.), Intelligent Data Analysis for Real-Life Applications: Theory and Practice., IGI Global, 2012, pp. 206–227, Ch. 11.

[41] E. Soria, J.D. Martín, C. Fernández, R. Magdalena, A.J. Serrano, Á. Moreno, Qualitative modelling of time series using self-organizing maps: application to animal science, in: Proceedings of the 6th WSEAS International Conference on Applied Computer Science, ACS'06, World Scientific and Engineering Academy and Society (WSEAS), Stevens Point, Wisconsin, USA, 2006, pp. 183–187.

[42] C. Fernández, E. Soria, J.D. Martín-Guerrero, A.J. Serrano, Neural networks for animal science applications: two case studies., Expert Systems with Applications 31 (2) (2006) 444–450.

[43] R. Magdalena, C. Fernández, J.D. Martín, E. Soria, M. Martínez, M.J. Navarro, C. Mata, Qualitative analysis of goat and sheep production data using self-organizing maps, Expert Systems 26 (2) (2009) 191–201.

[44] J. Vesanto, E. Alhoniemi, J. Himberg, K. Kiviluoto, J. Parviainen, Self-organizing map for data mining in matlab: the som toolbox, Simulation News Europe (25) (1999) 54.

[45] L. Cohen, Time Frequency Analysis., first ed., Prentice Hall PTR, New Jersey, USA, 1995.

[46] F.A. Atienza, J.L. Rojo-Álvarez, G. Camps-Valls, A.R. Mu noz, A. García-Alberola, Bootstrap feature selection in support vector machines for ventricular fibrillation detection, in: ESANN, 2006, pp. 233–238.

[47] F. Alonso-Atienza, J.L. Rojo-Álvarez, A. Rosado-Mu noz, J.J. Vinagre, A. GarcA-a-Alberola, G. Camps-Valls, Feature selection using support vector machines and bootstrap methods for ventricular fibrillation detection, Expert Systems with Applications 39 (2) (2012) 1956–1967.

[48] K. Kiviluoto, Topology preservation in self-organizing maps., in: IEEE International Conference on Neural Networks, 1996, vol. 1, 1996, pp. 294–299.